SOL-GEL SYNTHESIS OF VANADIUM PHOSPHORUS OXIDES AS CATALYST FOR THE PARTIAL OXIDATION OF BUTANE TO MALEIC ANHYDRIDE

Juan M Salazar, Keith L. Hohn[*]

Department of Chemical Engineering

Kansas State University

Manhattan, KS, USA

Introduction

The preparation of vanadyl pyrophosphate (VPO) strongly influences their catalytic activity in partial oxidation of butane to maleic anhydride[1,2]. The characteristics of $VOHPO_4 \bullet 0.5H_2O$, (called "the precursor" in this paper) are strongly influenced by the reagents, the ratio of phosphorous to vanadium, the nature of the solvent and the conditions of the reduction step during the preparation. Synhesis conditions can control the characteristics of the precursor and thus the catalytic behavior of $(VO)_2P_2O_7$, which will be referred to in this paper as the active phase[2].

Several techniques have been applied to increase the activity of VPO catalysts and they are summarized by Hutchings[3]. Particle morphology is also an important issue for the activity of the catalytic materials since crystallites with exposure of the (100) plane in the active phase are considered more selective[4,5]. Transformation from the precursor to the active phase is topotactic; the (001) plane on the former transforms into the (100) in the latter[6]. Thus, the morphology of the precursor plays an important role on the catalytic activity of VPO[5]. In their work Horowitz et al reduced $VOPO_4$ to the precursor by secondary or primary alcohols. It was found that the type of alcohol dramatically influenced the morphology of the particles and consequently their catalytic activity[5]. Therefore, synthetic routes that can be oriented to the manipulation of the precursor morphology, crystallite size and surface area are candidates to yield an improved catalyst.

[*] Corresponding Author, e-mail hohn@ksu.edu

Sol-gel methods have often been used to synthesize metal oxide catalysts and adsorbents due to their ability to regulate the composition and nanostructure of the final material during the earlier stages of synthesis[7]. The metal alkoxide method (MAM) is one of the most common sol-gel procedures. The application of the MAM to VPO has shown that reactions in aprotic solvents and in the absence of water benefit the formation of small and compact particles[8]. Other studies showed that the active phase could be synthesized through a sol-gel procedure and explored the application of colloidal and polymeric gelation to form membrane reactors[9]. Methods that involve the use of proton exchange resin are also reported in the synthesis of $VOPO_4 \bullet 2H_2O$ (a hydrated vanadium (V) phase)[10]. An important part of the sol-gel procedure, which for VPO has not been previously studied in any detail, is the procedure used to remove the solvent from the gel. This drying process can be carried out by evaporation or by the well known supercritical drying[11,12]. The process is carried out in an autoclave and an appropriate excess of solvent is added to reach the critical point before the gel loses the solvent[11]. Several transformations of the vanadium phosphorous oxides can occur during this process. Different compositions, morphologies and subsequently different catalytic properties are reported as consequences of the high-pressure synthesis of VPO[13,14,15].

Griesel et al found that high pressure and temperature preparations yielded active catalyst for the partial oxidation of n-butane. $VOPO_4 \bullet 2H_2O$ was reduced with 1-octanol at $150^{o}C$ in an autoclave generating 50% selectivity at 39% of conversion when evaluated at $400^{o}C$[14]. A precursor prepared by mixing V_2O_5, H_3PO_4, oxalic acid and water in an autoclave at $150^{o}C$ yielded an activated catalyst with 61% of selectivity at 35% of conversion after reacting at 400oC [16].

The purpose of this study is to apply a sol-gel technique, namely the MAM, followed by near supercritical drying in an autoclave in order to increase the surface area of VPO and to produce active and selective catalysts for butane oxidation.

Experimental Section

Sol-Gel Synthesis in THF. As a reference, the precursor was prepared according to one of the traditional methods[5]. The procedure is comprise of the reduction of V_2O_5 with a mixture of isopropyl and benzyl alcohol and the addition of the phosphoric acid, 85% (Fisher). The sol-gel procedure was based on the reported methodology by Ennacciri et al[17]. Two 1M solutions were prepared: (i) vanadium (V) triisopropoxide oxide (the alkoxide) (Alfa-Aesar) in tetrahydrofuran (THF) (Fisher) and (ii) orthophosphoric acid, anhydrous solid (Fluka), in THF (Fisher). Then equal volumes (10 ml) of each solution were mixed. The phosphoric acid solution (ii) was added to the alkoxide solution (i) while stirring. The gel was aged for three hours and the final slurry was dried according to the processes indicated below.

Drying Process. As a control procedure, the yellow slurry was dried under nitrogen at atmospheric pressure for four hours. This material was called AD. To dry the materials under high pressure a reported procedure was followed[18]. The slurry was poured into a glass-lined 600-ml capacity reactor (Parr). The reactor was pressurized with nitrogen to 7.9 bars, heated from 25^oC to 265^oC at a rate of $1^oC/min$. After ten minutes at the maximum temperature, the reactor was vented in about one to two minutes. In order to reach the critical point and avoid the collapse of the fragile gel, solvent was added before the slurry was dried in the autoclave[11]. To determine the influence of the amount of added solvent in the final product an experiment with a completely randomized design was carried out with three levels or treatments: adding 20 ml, 50 ml or 100 ml (low, medium and high level, respectively) of THF. The resultant materials were called LS, MS and HS respectively. Three replications were performed for each level. The extra solvent was also evaluated as a mixture of isopropanol and THF.

Catalytic Evaluation. Precursors LS, MS and HS were evaluated as catalysts for the partial oxidation of Maleic Anhydride. The amount of catalyst and the total gas flows were adjusted to have gas hourly space velocities (GHSV) from 1700 h^{-1}to 2200 h^{-1}. The

precursors were initially treated under nitrogen from 298 K to 673 K and remained at this temperature for 2 h. While kept at 673 K, a reacting mixture of 1.7% butane in air was flowed through the catalytic bed; the reaction was carried out for 72 h. The products were analyzed with gas chromatography employing a 5Å molecular sieve and a Porapaq QS column; the separated products were analyzed with a thermal conductivity detector (TCD) and a flame ionization detector (FID). The activated materials were called CLS, CMS and CHS.

Characterization. Diffuse reflectance infrared Fourier transform spectroscopy (DRIFTS) was done with a Thermo Nicolet Nexus™ 670 FT-IR spectrophotometer equipped with a Smart Collector. The samples were diluted to 1-10 weight % in potassium bromide infrared grade (Acros). X-ray diffraction (XRD) was carried out with a Bruker axs D8 advance diffractometer that was set at 40 kV and 40 mA. Scans were from 50 to 700 (2θ) with a step size of 0.050 and 1.5 s/step. The diffractometer radiation was copper Kα (λ=1.54Å). The sample was put on the sample holder and exposed to the atmosphere at room temperature during the analysis. The scanning electron micrographs (SEM) were taken with a Hitachi S-3500N. The surface areas of the samples were determined by an Altamira instruments AMI-200 according to the BET model. The oxidation state of the vanadium in the samples was determined with the volumetric method reported in the literature[19].

Results and Discussion

Sol-Gel Synthesis in THF. The sol-gel procedure resulted in an immediate gelation process and an orange gel was observed. After three hours of reaction the mixture turned into bright yellow slurry. The surface area of the slurry following atmospheric drying is 56 m^2/g. The X-ray diffraction pattern of the dried compound, Figure 1, shows the presence of many of typical reflections of α-$VOPO_4$ as well as some of the reflections of $VOPO_4•2H_2O$[6] Table 1. However, there are other very important reflections at 8.71Å, 5.03Å and 2.91Å that are not characteristic of any of the most well known VPO phases. These reflections are attributed to the intercalation of either solvent or isopropyl alcohol.

Okuhara and coworkers recently explored the phenomena of exfoliation by means of intercalating alcohols into the layers of $VOPO_4 \cdot 2H_2O$. The process was carried out for three hours at relatively low temperatures (30-70°C) and the subsequent reduction of the exfoliated VPO by primary alcohols yielded the precurso[20]. Previous works employed alkylphosphonic acid that reacted with V_2O_5 to intercalate the corresponding alkyl groups and intercalated pyridine into $VOPO_4 \cdot 2H_2O$ by reflux[21,22].
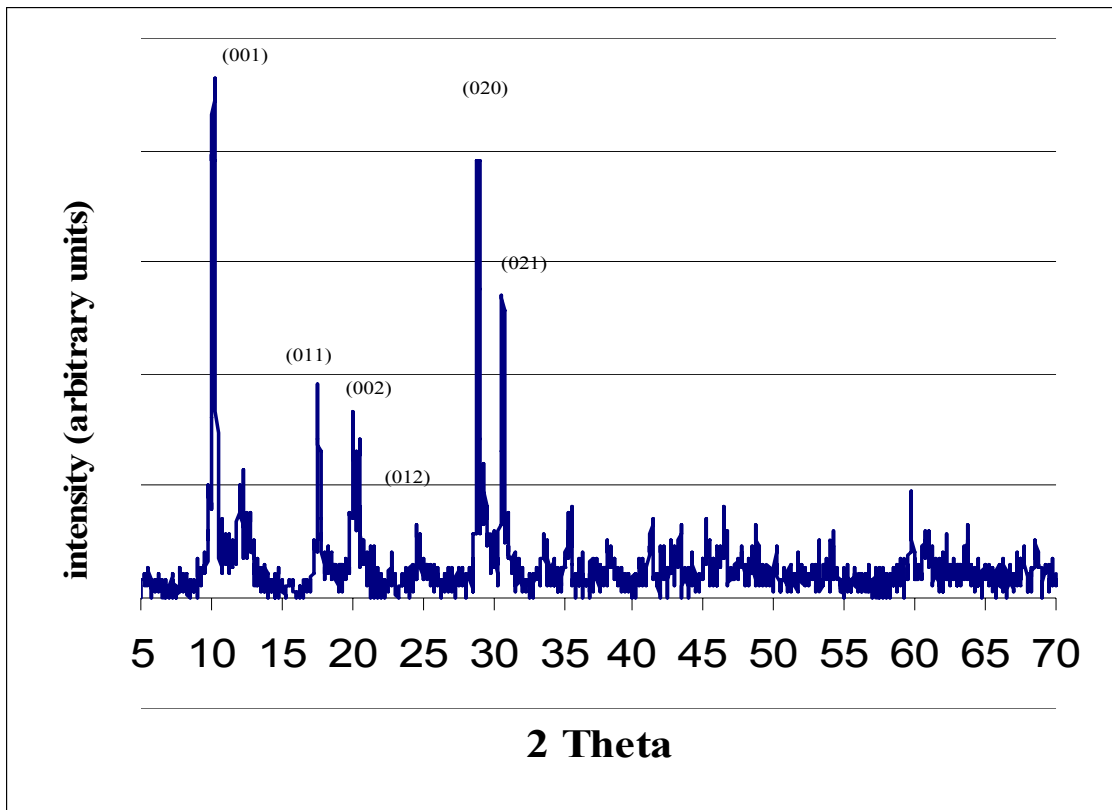
Figure 1 XRD pattern of VPO slurry after drying in a stream of nitrogen.

Table 1 XRD spacing in Å (Relative Intensity)

Atmospheric Drying		
Ref. Compounds		This work
R3[6]	R2[6]	AD
		8.71 (100)
	7.45 (vS)	7.32 (21.5)
		5.03 (40.9)
4.43 (w)		4.41 (35.5)
3.57 (S)		3.59 (11.8)
3.07 (vS)	3.1 (M)	3.07 (83.9)
		2.91 (58.1)
	2.19 (w)	2.18 (15.1)
1.9 (S)		1.95 (12.9)
1.83 (M)		1.87 (14)
1.56 (M)	1.55 (S)	1.55 (20.4)
1.5 (M)	1.52 (S)	1.52 (13.4)
1.43 (M)	1.46 (M)	1.46 (13.8)

R2: $VOPO_4 \cdot 2H_2O$, R3: $VOPO_4$, vS: Very strong, S: strong, M: Medium, w: Weak

Autoclave Drying. The pressure in the autoclave was measured for three levels of solvent (100 ml, 50 ml and 20 ml) as a function of temperature and is shown in Figure 2. For comparison, a theoretical curve of the liquid-vapor equilibrium of THF is also plotted[23]. For the preparation of MS and HS the system develops a behavior similar to the vapor-liquid equilibrium of pure solvent and the liquid vaporizes very close to the critical point. In contrast, when LS precursor is to be prepared the liquid completely vaporizes and never reaches the critical point.
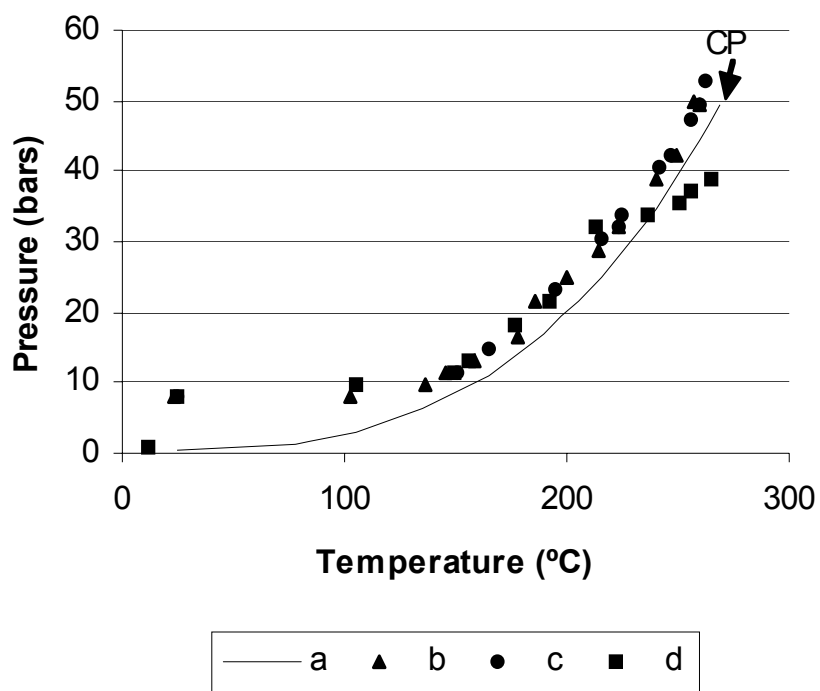
Figure 2 Pressure-temperature behavior during the autoclave drying compared with the vapor pressure of THF. a) Vapor pressure of pure THF b) High amount of solvent (100 ml) c) Medium amount of solvent (50 ml) d) Low amount of solvent (20 ml). CP: Critical Point.

Surface Area Measurements of Precursors. The influence of the amount of added solvent in this parameter is determined by the analysis of variance for an experiment with three levels of solvent and results in the conclusion that there is no statistical difference between MS and HS, but LS is statistically different from the average of HS and MS. The Bonfferoni t test[24] was used to compare means in Table 2. The values are also higher than the results reported by Ennaciri for atmospheric pressure drying in air[17]. These results indicate that vaporization of the solvent during drying before the critical point leads to a dramatic loss of surface area.

Table 2 BET Surface areas for the products dried after adding the three amounts of solvent

Precursor	Average Surface Area (m^2/g)
LS	65
MS	102
HS	121

XRD analysis of precursors. X-ray diffraction patterns were obtained for the materials dried with different amounts of solvent. The amount of added solvent in the three cases influences the chemical composition of the final materials. Figure 3 a) and e) are X-ray diffraction patterns of the sample shown in Figure 1 and the precursor respectively[6]. The crystallography of the resultant materials Figure 3 b) through d) evidences the transformation of the $VOPO_4$ phase into a compound that can be identified as the precursor.
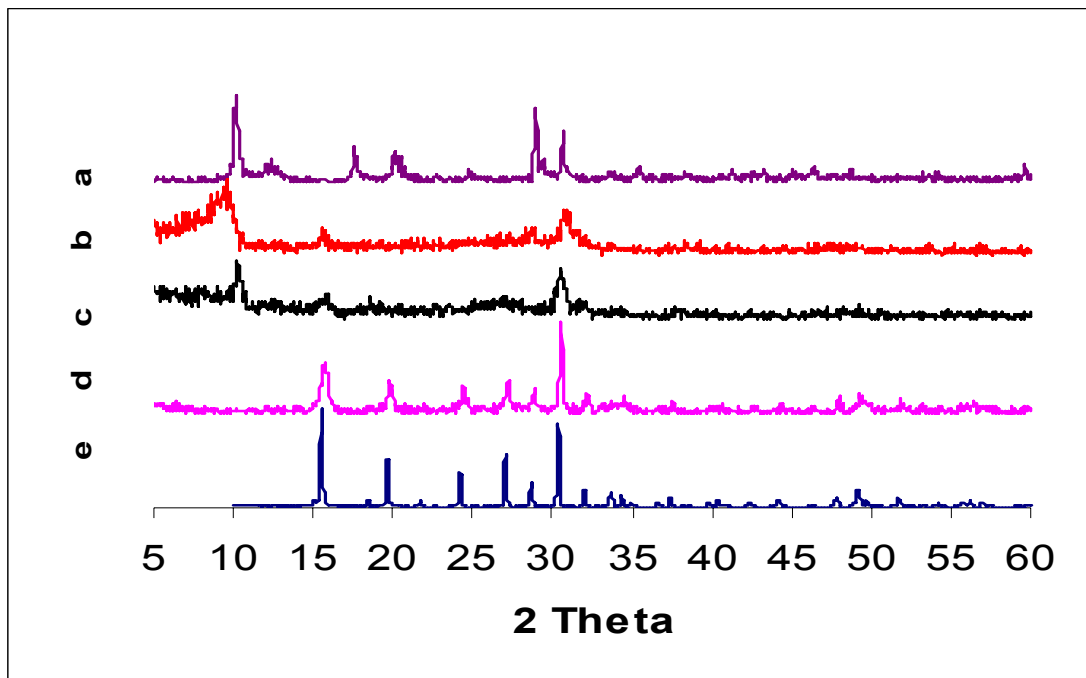
Figure 3 XRD patterns of different VPO materials a) Slurry dried on nitrogen b) High amount of solvent c) Medium amount of solvent d) Low amount of solvent e) $VOHPO_4 \bullet 0.5H_2O$.

These results show that in addition to the physical changes that occur during autoclave drying, chemical transformations also occur. Interestingly, while the materials dried after adding high and medium amounts of solvent had nearly the same surface area, they have quite different phase compositions. This suggests that the differences in surface area for these materials are not just due to differences in phase composition: the autoclave drying procedure has a substantial role in producing high surface-area vanadium phosphates.

Reduction process inside the autoclave. As discussed in the previous sections, when the material was dried inside the autoclave, chemical transformations occurred, which yielded products containing reduced-vanadium phases. The reduction process can be attributed to the alcohol generated as byproduct during the hydrolysis of the vanadium alkoxides. It is known that alcohols are good reducing agents to prepare the precursor[25]. Reduction of $VOPO_4$ with isopropyl alcohol and other alcohols has been reported to yield non-agglomerated particles with platelet crystalline morphology as the results of the reduction of $VOPO_4$[5]. As more solvent was added to the slurry the concentration of

9

alcohol decreased and fewer reduced products were obtained. In contrast, low amount of added solvent resulted in more reduced phases. As calculated from surface area measurements, crystallite thickness can be similar to that calculated from XRD analysis. This is an indication that the homogeneity and morphology of the material correspond to $VOHPO_4 \bullet 0.5H_2O$. When there is not agreement between the two calculations the presence of some impurities can be implied and the degree of reduction can be elucidated. It is interesting to notice that the particle size of the precursors after the drying step, as observed by SEM, is similar of those obtained by Okuhara and coworkers[26]. Their claims include the formation of platelets of the reduced compounds with particle sizes of 500-6000 nm in length and 69-156 nm in thickness (calculated from surface area measurements). The SEM- estimated crystallite sizes of the reduced precursor MS and HS are approximately 400 nm in length and for LS is 500 nm. In this work, the thickness of crystallites from the measured surface area was calculated only for LS precursor since it is thought to have the highest concentration of $VOHPO_4 \bullet 0.5H_2O$. Surface-area based estimation of LS precursor is about 9 nm and the estimation from the (001) plane reflection of Figure 3 d) is 17 nm, indicating that the assumption of pure compound for the surface area estimation is not held for this precursor. To increase the concentration of this compound in the precursors, isopropanol was added as the extra solvent and was aged for 15 hours previous the drying step. The thickness of LS precursor estimated from the Scherer's equation[16] and the XRD analysis shown in Figure 4. The SEM analysis of these samples allowed the estimation of crystallites lengths from 700 to 1100 nm and from the surface area measurement the thickness was estimated from 14 to 18 nm while Scherer's equation yielded from 12 to 18 nm. These estimations imply that the concentration of hemihydrate was increased with the addition of isopropanol as part of the extra solvent.
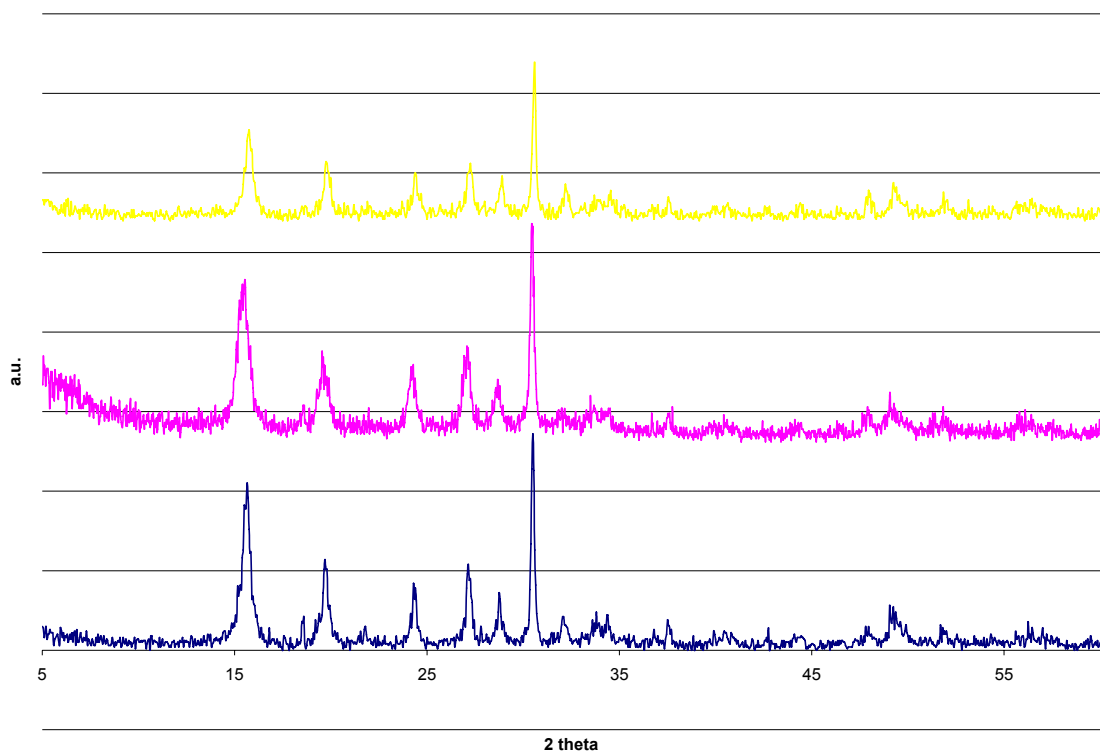
Figure 4 XRD patterns of precursors dried in autoclave with a) 20 ml of THF b) 40 ml of isopropanol and 10 ml of water and c) 20 ml of isopropanol and 30 ml of water.

Catalytic evaluation. LS, MS and HS precursors were evaluated as catalysts and compared to a control synthesized through the traditional methodology[5]. Results are shown in Table 3. At approximately similar levels of conversion, the selectivity shows the tendency to increase when the amount of solvent used during the precursor's drying decreases. These results are attributed to the higher concentrations of the precursor when less solvent was used. After the reaction tests their XRD patterns have reflections typically present in the active phase[6], Figure 5. The scanning electron micrographs in Figure 6 illustrate the morphology of these materials. Small non agglomerated crystallites of about 600 nm in length are observed as activated catalysts from LS precursor. The crystallite thickness was estimated from both the Scherer's equation[16] and the surface area[26]. The XRD-based calculation yielded 14 nm; the estimation from the surface area measurements gave values of 4 nm. This, again, suggests that the assumption in

11

homogeneity of the surface-area-based calculation is not valid for these materials; it also suggests that there are other vanadium phosphates in addition to the hemihydrate. The similar values for intrinsic activity in Table 3 suggest the presence of an active surface with very selective domains since the surface of those domains is able to yield about the same amount of maleic anhydride as the highly concentrated pyrophosphate. Selective parts of the activated catalysts are suspected to be the very small particles present in Figure 6 b) produced by breaking down the corresponding precursor a). The existence of the non-selective low surface area domains is the reason for their low selectivity at the evaluated level of conversion (compared to those reported in the literature for small crystallites of the activated catalyst).

Table 3 Catalytic performance of Autoclave dried samples.

Treatment	Butane Conversion	Maleic Anhydride selectivity	Intrinsic activity 10^{-5} Mol MA/m^2/h
Traditional	37.42	28.65	1.82
Low solvent	31.05	41.76	1.01
Medium Solvent	20.58	27.99	1.73
High Solvent	28.36	12.07	1.07
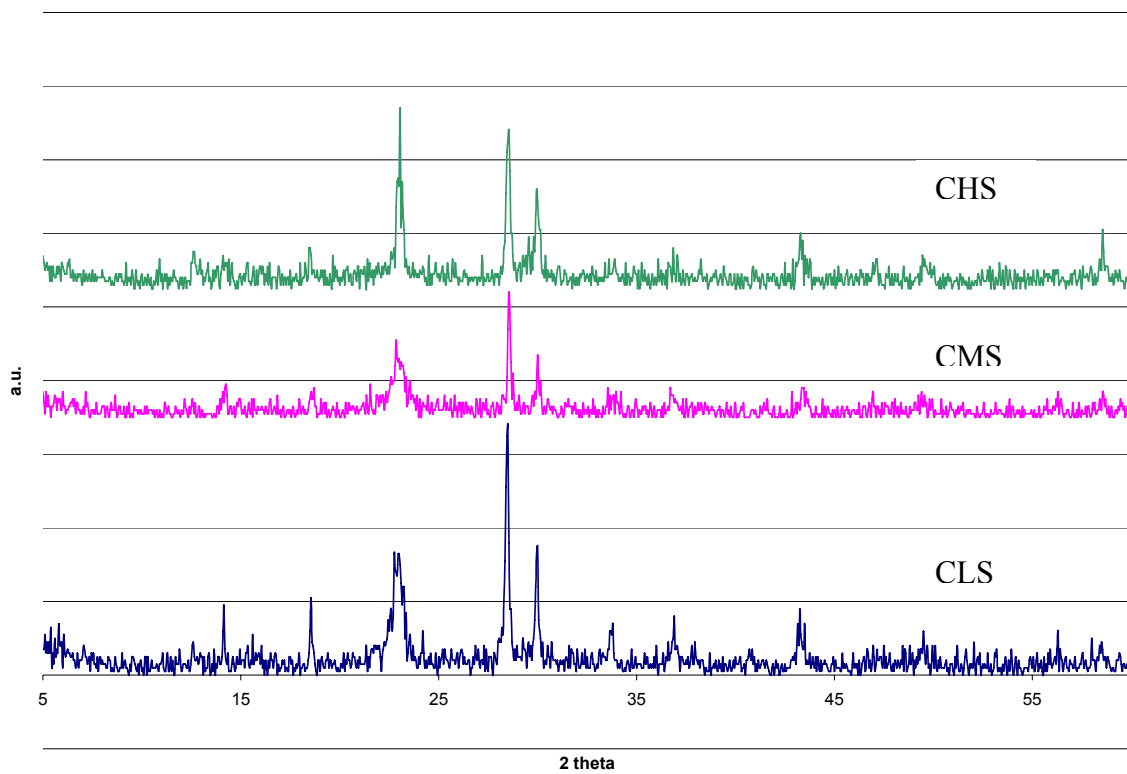
Figure 5 XRD patterns of activated catalysts from the precursors prepared with the three levels of extra solvent.
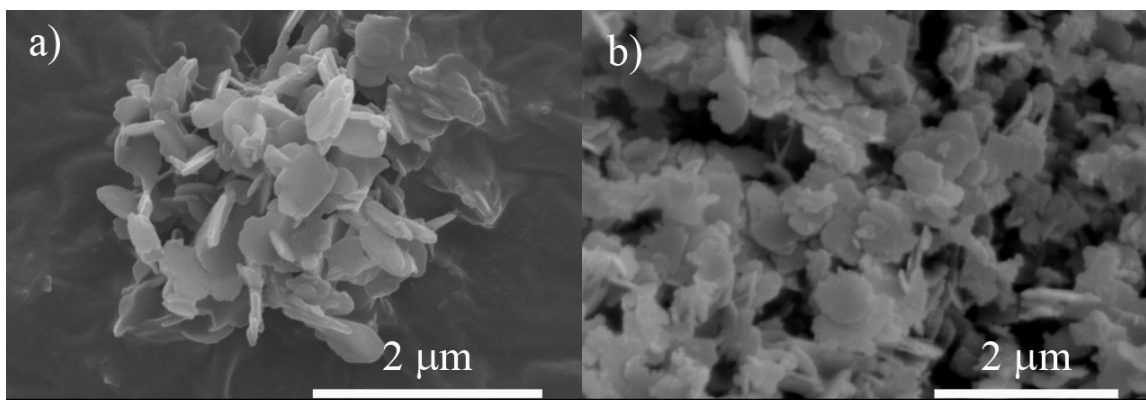
Figure 6 Scanning electron micrographs of a) precursor and b) activated catalysts prepared with the sol-gel route and autoclave drying with low amount of extra solvent.

Conclusion

A gelation process leads to production of hydrated and dehydrated α-VOPO$_4$, and some intercalated compounds. Drying these compounds at near supercritical conditions is a suitable procedure to produced improved materials since it leads to the precursor with well developed (001) plane.

The surface areas are dramatically affected by the amount of solvent added to the slurry, since it influences the final pressure of the autoclave. When the amount of solvent is doubled the surface area is also doubled. The amount and composition of such a solvent also affect the reduction process inside the autoclave. The composition of the obtained products changes from the intercalated VOPO$_4$ phase towards the precursor when the amount of solvent is reduced in 80%.

The sol-gel prepared precursors resulted in selective small crystallites of vanadyl pyrophosphate.

References

1. Hodnett, B. K. *Catalysis Reviews - Science and Engineering* **1985**, *3,* 373-424.

2. Centi, G.; Cavani, F.; Trifiro, F.; Editors **2001**, 505.

3. Hutchings, G. J. *Journal of Materials Chemistry* **2004**, *23,* 3385-3395.

4. Centi, G.; Trifiro, F.; Ebner, J. R.; Franchetti, V. M. *Chemical Reviews (Washington, DC, United States)* **1988**, *1,* 55-80.

5. Horowitz, H. S.; Blackstone, C. M.; Sleight, A. W.; Teufer, G. *Applied Catalysis* **1988**, *2,* 193-210.

6. Bordes, E. *Catalysis Today* **1987**, *5,* 499-526.

7. Yan, C.; Sun, L.; Cheng, F. *Handbook of Nanophase and Nanostructured Materials* **2003**, 72-101.

8. Higgins, R.; Hutchings, G. J. United States of America Patent 4,317,777, 1982.

9. Farrusseng, D.; Julbe, A.; Lopez, M.; Guizard, C. *Catalysis Today* **2000**, *1-3,* 211-220.

10. R'kha, C.; Vandenborre, M. T.; Livage, J.; Prost, R.; Huard, E. *Journal of Solid State Chemistry* **1986**, *2,* 202-215.

11. Pierre, A. C.; Editor **1998**, 394.

12. Teichner, S. J. *Springer Proceedings in Physics* **1986**, *Aerogels,* 22-30.

13. Griesel, L.; Bartley, J. K.; Wells, R. P. K.; Hutchings, G. J. *Catalysis Today* **2005***, 1-2,* 131-136.

14. Dong, W.; Bartley, J. K.; Dummer, N. F.; Girgsdies, F.; Su, D.; Schloegl, R.; Volta, J.; Hutchings, G. J. *Journal of Materials Chemistry* **2005***, 31,* 3214-3220.

15. Griesel, L.; Bartley, J. K.; Wells, R. P. K.; Hutchings, G. J. *Journal of Molecular Catalysis A: Chemical* **2004***, 1,* 113-119.

16. Taufiq-Yap, Y. H.; Hasbi, A. R. M.; Hussein, M. Z.; Hutchings, G. J.; Bartley, J.; Dummer, N. *Catalysis Letters* **2006***, 3-4,* 177-181.

17. Ennaciri, S. A.; Malka, K.; Louis, C.; Barboux, P.; R'kha, C.; Livage, J. *Phosphorus Research Bulletin* **2000**, 87-93.

18. Utamapanya, S.; Klabunde, K. J.; Schlup, J. R. *Chemistry of Materials* **1991***, 1,* 175-181.

19. Nakamura, M.; Kawai, K.; Fujiwara, Y. *Journal of Catalysis* **1974***, 3,* 345-355.

20. Yamamoto, N.; Hiyoshi, N.; Okuhara, T. *Chemistry of Materials* **2002***, 9,* 3882-3888.

21. Johnson, J. W.; Jacobson, A. J.; Brody, J. F.; Rich, S. M. *Inorg. Chem.* **1982***, 10,* 3820-3825.

22. Johnson, J. W.; Jacobson, A. J.; Brody, J. F.; Lewandowski, J. T. *Inorg. Chem.* **1984***, 24,* 3842-3844.

23. Poling, B. E.; Prausnitz, J. M.; O'Connell, J. P. *The properties of gases and liquids 5th ed.* McGraw-Hill: New York, 2001; Vol. 1, pp 768-p A-50.

24. Kuehl, R. O. *Design of experiments: statistical principles of research design and analysis 2nd ed.* Brooks/Cole: Pacific Grove: Pacific Grove, 2000; Vol. 1, pp 666-94.

25. Busca, G.; Cavani, F.; Centi, G.; Trifiro, F. *Journal of Catalysis* **1986**, *2,* 400-414.

26. Kamiya, Y.; Ueki, S.; Hiyoshi, N.; Yamamoto, N.; Okuhara, T. *Catalysis Today* **2003**, *1-4,* 281-290.